



NTNU
Norwegian University of Science and Technology
Faculty for Engineering Science and Technology
Department of Petroleum Engineering and Applied Geophysics

DIPLOMA THESIS

Compressibility and Sound Speed

Vidar Åseng,
Trondheim
February 2006



NTNU
Norges teknisk- naturvitenskapelige universitet
Fakultet for ingeniørvitenskap og teknologi
Institutt for petroleumsteknologi og anvendt geofysikk

MASTEROPPGAVEN

Kandidatens navn: *Vidar Åseng, f. 29.04.78*

Oppgavens tittel: *Kompressibilitet og lydhastighet*

Studieretning: *Petroleumsteknologi*

Fagområde: *Produksjon*

Tidsrom: *september 05 – februar 06*

Veileder: *Prof. J.S. Gudmundsson*

.....Vidar Åseng (sign.).....

Trondheim, 17.02.06

Table of contents

Table of contents	0
1 Introduction	3
2.1 Introduction to compressibility	4
2.2 Vazquez and Beggs correlation.....	5
2.3 Petrosky and Farshad correlation	5
2.4 Al-Marhoun correlation.....	6
2.5 Undersaturated oil compressibility.....	6
2.6 Water isothermal compressibility.....	7
2.7 Gas compressibility	7
3 Compressibility in multiphase mixtures.....	10
3.1 Two-phase isothermal compressibility.....	10
3.2 Isentropic compressibility	11
3.3 Ratio of specific heats	11
4 Speed of sound	13
4.1 Introduction	13
4.2 NTNU sound speed model	13
4.3 Speed of sound in oils	16
4.4 Sound speed in dead oils	16
4.5 Sound speed in live oil	17
4.6 Sound speed in oil under bubblepoint pressure.....	17
5 Discussion	19
6 Conclusion.....	20
Nomenclature	21
References	22
Tables	24
Figures.....	27

1 Introduction

The acoustic velocity in pure fluids and fluid mixtures is an important parameter for several areas in the petroleum industry. Seismic exploration, well testing, logging and metering are some of these areas.

Pressure Pulse technology is used to measure the rate of fluids produced by wells and flowing in pipelines, and to detect and monitor deposits in these as well. The technology was developed by Gudmundsson (1998) as described by Celius and Gudmundsson (1999). A basic part in this technology is a theoretical model for sound speed in multi-phase mixtures developed at NTNU (Dong and Gudmundsson, 1993). In this model the velocity in the mixture is directly connected to the properties of its constituents.

Alternative models can be used in sound speed estimations. One approach is to use semi-empirical correlations used in the petroleum industry for estimation of the compressibility in gas, oil, water and mixtures of these. Such models should be tested out and compared to the NTNU sound speed model.

The compressibility of a fluid is closely related to its acoustic velocity. Empirical correlations for compressibility in mixtures or in each of its constituents exist in the literature. The relations between acoustic velocity and compressibility can be used to make these correlations useable in sound speed models. Comparison is made between these correlations and the NTNU model in the thesis work.

Heat capacities are also important parameters in the NTNU sound speed model. Assumptions are made towards the heat capacity parameters in the model. These assumptions have been tested using the process simulation tool Hysys for estimation of fluid properties

2 Single phase isothermal compressibility

2.1 Introduction to compressibility

The compressibility coefficient is directly connected to the determination of speed velocities in fluids. The isothermal compressibility of a single-phase fluid is defined as the volumetric change when pressure is changed and temperature held constant:

$$c_T = -\frac{1}{V} \left(\frac{\partial V}{\partial p} \right)_T, \quad (1)$$

where V is the system total fluid volume.

Several empirical correlations for estimating fluid PVT properties have been developed in the petroleum industry. The well-known correlations from Standing for bubble point pressure, solution gas-oil ratio, and oil formation volume factor, are the basis for many other works later on. Correlations for compressibility have been developed for gas, oil and water (brine), and also multi-phase.

The first models for estimating undersaturated isothermal oil compressibility were graphical. Calhoun's (1947) method related a value of average compressibility to the oil relative density at bubble point pressure. In 1957, Trube used pseudoreduced pressure and temperature to determine undersaturated oil compressibility graphically. The three methods I have chosen to have a closer look on in this thesis are all empirical methods for estimating oil compressibility above bubble point pressure. Vazquez and Beggs (1980) worked out a set of correlations using available reservoir parameters. The oil compressibility was estimated as a function of R_s , T , γ_o , γ_g , and p . The same parameters were used by Petrosky and Farshad (1993) to make an improved equation for estimating isothermal oil compressibility. The third method considered here, was developed by Al-Marhoun (2003).

Fewer methods have been developed for determining oil compressibility at pressures below the bubble point. McCain (1988) developed a correlation including p_b and dropping γ_g as

parameters compared to the methods for undersaturated oils, also providing correlations for when bubble point pressure or solution GOR is not known.

2.2 Vazquez and Beggs correlation

Vazquez and Beggs (1980) gave equations for estimating solution gas-oil-ratio and oil formation volume factor. To estimate the oil FVF for pressures above the bubble point pressure, a correlation for oil compressibility was developed. They used more than 4000 data points in a linear regression model to obtain the equation:

$$c_o = \frac{(a_1 + a_2 R_s + a_3 T + a_4 \gamma_{gs} + a_5 \gamma_o)}{a_6 p}, \quad (2)$$

where

$$a_1 = -1433.0$$

$$a_2 = 5.0$$

$$a_3 = 17.2$$

$$a_4 = -1180.0$$

$$a_5 = 12.61$$

$$a_6 = 10^5$$

and

$$\gamma_{gs} = \gamma_{gp} \left(1 + 5.912e10^{-5} \gamma_o \times T \times \log \frac{p}{114.7} \right),$$

where γ_{gs} is the gas specific gravity that would result from separator conditions of 100 psi and γ_{gp} is the gas specific gravity obtained at separator conditions of T and p. With c_o in psi^{-1} , p in psi and T in $^{\circ}\text{F}$.

2.3 Petrosky and Farshad correlation

Petrosky and Farshad's work (1993) included empirical correlations for bubblepoint pressure, solution gas-oil ratio and oil formation volume factor as well as undersaturated isothermal oil compressibility. They developed the correlations from 81 PVT laboratory analyses of Gulf of Mexico fluid samples. Although the model was developed specifically for Gulf of Mexico crude it can also be considered for use in other regions. They also compared their model to

Vazquez and Beggs, finding theirs was more accurate. The oil compressibility correlation was developed based on the same independent variables as Vazques and Beggs used in their correlation:

$$c_o = 1.705e^{-7} R_s^{0.69357} \gamma_g^{0.1885} \gamma_o^{0.3272} T^{0.6729} p^{-0.5906} \quad (3)$$

with R_s in scf/STB, T in °F, p in psi and c_o in psi^{-1} .

2.4 Al-Marhoun correlation

Al-Marhoun (2003) used 3412 data points from analyses of fluids from the Middle East to develop his empirical correlation for the oil compressibility. This model was tested against the two previously mentioned methods, concluding it outperforms them based on low value of average absolute error and standard deviation. Al-Marhoun chose other parameters than the two previous works for estimating the compressibility. The reason for this was that he found that different flash separation laboratory tests gave different combinations of data for R_s , γ_g and γ_o . This resulted in different values for the compressibility of a given crude oil at the same reservoir conditions. Because of this Al-Marhoun defined the parameter γ_{ob} and using it as a variable in the equation for estimating c_o :

$$c_o = -14.1042 + \frac{2.7314}{\gamma_{ob}} - \frac{56.0605(p - p_b)}{\gamma_{ob}^3} - \frac{580.8778}{T + 460} \quad (4)$$

where

$$\gamma_{ob} = \frac{\gamma_o + 2.18e^{-4} R_s \gamma_g}{B_{ob}} \text{ is the bubblepoint oil relative density,}$$

with c_o in psi^{-1} , p in psia, T in °F, R_s in scf/STB, γ_o relative to water density

2.5 Undersaturated oil compressibility

Fewer publications have been made regarding correlations for the oil compressibility at pressures below the bubblepoint pressure. The definition of the oil compressibility below the bubblepoint pressure is:

$$c_o = -\frac{1}{B_o} \frac{\partial B_o}{\partial p} + \frac{B_g}{B_o} \frac{\partial R_s}{\partial p} \quad (5)$$

Ramey (1964) published empirical correlations for the compressibility of oils below the bubblepoint pressure. An empirical model was developed by McCain & al. (1988) using test data of black oils from 260 well locations worldwide. Three models were developed, one for when all input parameters is known, and the last two for cases where the bubblepoint pressure and solution GOR is not available. When all the wanted variables are known this equation can be used for the best result:

$$\ln c_o = -7.573 - 1.450 \ln p - 0.383 \ln p_b + 1.402 \ln T + 0.256 \ln \gamma_o + 0.449 \ln R_{sb} \quad (6)$$

with c_o in psi^{-1} , p in psia, T in $^{\circ}\text{R}$, γ_o in $^{\circ}\text{API}$ and R_{sb} in scf/STB.

2.6 Water isothermal compressibility

For systems containing water (brine) correlations are needed to express the water compressibility. An equation for estimating water isothermal compressibility was proposed by Brill and Beggs (1978) as shown by Ahmed (2001). No corrections for dissolved gas and solids are made in this method though:

$$c_w = (C_1 + C_2 T + C_3 T^2) \times 10^{-6} \quad (7)$$

where the constants C_1 , C_2 and C_3 are pressure dependant:

$$C_1 = 3.8546 - 0.000134 p$$

$$C_2 = -0.01052 + 4.77 \times 10^{-7} p$$

$$C_3 = 3.9267 \times 10^{-5} - 8.8 \times 10^{-10} p$$

with T in $^{\circ}\text{F}$, p in psia and c_w in psi^{-1} .

2.7 Gas compressibility

The isothermal gas compressibility is defined by the same equation for change in volume when pressure changes, as the liquid phases:

$$c_g = -\frac{1}{V} \left(\frac{\partial V}{\partial p} \right)_T \quad (8)$$

The gas isothermal compressibility is of greater magnitude than compressibility in liquid phases. It is also more dependent on pressure and temperature changes. Muskat (1949) combined the real gas law with the above definition, giving this relationship for the gas compressibility:

$$c_g = \frac{1}{p} - \frac{1}{z} \left(\frac{\partial z}{\partial p} \right)_T \quad (9)$$

A rough estimate of the isothermal gas compressibility can be made by assuming an ideal gas. Then $z = 1$ and the derivative $(\partial z / \partial p)_T = 0$, giving $c_g = 1/p$. According to Whitson and Brulé (2000) this is a reasonable approximation for sweet natural gas (not containing H₂S) at pressures less than about 1000 psia (≈ 69 bara).

The concept of pseudo-reduced compressibility was introduced by Trube in 1957, according to Ghedan & al. (1991), defined as the product of c_g and the pseudo critical pressure of the gas. This made a connection between the gas compressibility and Standing and Katz z-factor chart:

$$c_{pr} = c_g p_{pc} = \frac{1}{p_{pr}} - \frac{1}{z} \left(\frac{\partial z}{\partial p_{pr}} \right)_{T_{pr}} \quad (10)$$

The term $(\partial z / \partial p_{pr})_{T_{pr}}$ can be calculated from the well known Standing-Katz z-factor chart.

Ghedan & al. (1991) is also listing several examples of the Standing-Katz compressibility factor chart being expressed in equation form. While the earlier methods for gas compressibility calculations were using graphical methods, this made it possible to calculate it

empirically. Such an empirical method was shown by Ghedan & al. (1991), expressing the z-factor with the Dranchuk and Abou-Kassem (1975) method:

$$z = 1 + \left(A_1 + \frac{A_2}{T_{pr}} + \frac{A_3}{T_{pr}^3} + \frac{A_4}{T_{pr}^4} + \frac{A_5}{T_{pr}^5} \right) \rho_{pr} + \left(A_6 + \frac{A_7}{T_{pr}} + \frac{A_8}{T_{pr}^2} \right) \rho_{pr}^2 - A_9 \left(\frac{A_7}{T_{pr}} + \frac{A_8}{T_{pr}^2} \right) \rho_{pr}^5 + A_{10} (1 + A_{11} \rho_{pr}^2) \frac{\rho_{pr}^2}{T_{pr}^3} \exp(-A_{11} \rho_{pr}^2) \quad (11)$$

Differentiating this equation gives an expression for $(\partial z / \partial \rho_{pr})_{T_{pr}}$. To relate this partial derivative to $(\partial z / \partial p_{pr})_{T_{pr}}$, the reduced density equation is used:

$$\rho_{pr} = \frac{0.27 p_{pr}}{z T_{pr}} \quad (12)$$

By differentiating (NUM12) and substituting Ghedan & al. get this equation for reduced compressibility:

$$c_g p = 1 - \frac{p_r}{z T_r} \left(\frac{0.27 (\partial z / \partial \rho_r)_{T_{pr}}}{z + \rho_r (\partial z / \partial \rho_r)_{T_{pr}}} \right) \quad (13)$$

As mentioned, the term $(\partial z / \partial \rho_{pr})_{T_{pr}}$ can be found by differentiating equation (12). Then the gas compressibility can be determined from the reduced compressibility.

3 Compressibility in multiphase mixtures

3.1 Two-phase isothermal compressibility

When phases are mixed (gas/oil/water) the isothermal compressibility is often expressed as (Firoozabadi 1999):

$$c_m^T = S_g c_g^T + S_o c_o^T + S_w c_w^T \quad (14)$$

where c_m^T is the multiphase compressibility and S is the saturations of the different phases. When there is mass transfer between the phases, this equation is no longer valid. Close to the bubblepoint in the two-phase gas-oil region for example, this equation says that the two-phase compressibility is close to the oil compressibility. As showed by Firoozabadi (1999) even the smallest appearance of gas bubbles will increase the two-phase compressibility significantly, compared to the compressed liquid just before gas phase develops. The gas compressibility is higher than the liquid compressibility, but the two-phase compressibility can even be higher.

A set of equations to calculate the two-phase isothermal compressibility was developed by Firoozabadi & al. (1988). They started from the expression for the total volume (V_t) of gas (V_g) and liquid (V_l) combined:

$$V_t = V_g + V_l = \frac{RT}{p} \sum_{j=1}^2 z_j n_{j,t} \quad (15)$$

where $n_{j,t}$ is the total number of moles in phase j .

Further the derivative of equation (15) was taken, holding temperature and total number of moles constant:

$$\left(\frac{\partial V_t}{\partial p} \right)_{T,n} = -\frac{RT}{p^2} \sum_{j=1}^2 z_j n_{j,t} + \frac{RT}{p} \sum_{j=1}^2 \left[n_{j,t} \left(\frac{\partial z_j}{\partial p} \right)_{T,n} + z_j \left(\frac{\partial n_{j,t}}{\partial p} \right)_{T,n} \right] \quad (16)$$

From material balance equations, EOS' and equilibrium conditions, the sufficient number of equations is given to compute the unknowns, finally giving the isothermal compressibility from the equation above.

3.2 Isentropic compressibility

Firoozabadi and Pan (2000) developed a method for computing the isentropic compressibility. The isentropic single-phase compressibility is defined as volume changes with pressure changes along a thermodynamic path of constant entropy (S):

$$c_s = -\left(\frac{1}{V}\right)\left(\frac{\partial V}{\partial p}\right)_{S,n} \quad (17)$$

where V is the volume, S the entropy and n is the composition vector. n is defined by $n = (n_1, n_2, \dots, n_c)$, where c is the total number of components and n_i is the number of moles of component *i*. The expression for the two-phase isentropic compressibility is similar. In their work, Firoozabadi and Pan used the pressure in the liquid phase, rather than the gas phase. In this way the capillary pressure is taken into account. When the gas phase pressure equals the liquid phase pressure the interface between the two phases is flat, and there is no capillary pressure.

3.3 Ratio of specific heats

The isothermal and the isentropic compressibilities are related by the heat capacity ratio in this manner:

$$c_T = \left(\frac{C_p}{C_v}\right)c_s = \gamma c_s \quad (18)$$

Firoozabadi and Pan (2000) explain the application of the two compressibilities in reservoir engineering as c_T representing the fluid compressibility in the reservoir away from the well. In the wellbore temperature changes can occur due to pressure dropping, making the process no longer isothermal. c_s can therefore perhaps better represent the pressure and volume changes

in the wellbore, neglecting the temperature changes in the process (Firoozabadi and Pan, 2000). Since $C_p \geq C_v$, the isothermal compressibility is always higher than (or equal to) the isentropic.

In the Dong and Gudmundsson (1993) model for multi-phase sound speed (see section 4.2) it is assumed that the heat capacities of the oil are equal, making $\gamma = C_{p_o}/C_{v_o} = 1$. This assumption is also made in this study when estimating the sound speed from the three isothermal compressibility correlations.

The approximation of $C_{p_o} = C_{v_o}$ can be an uncertainty. I have therefore tested this approximation of $\gamma=1$ in the oil phase for some North Sea hydrocarbon mixtures in the Hysys simulation programme (see appendix B). Tables 1 to 4 show the specific heat ratio in the different phases and in the total mixture for four fluids from simulations in Hysys. The compositions of the fluids are listed in appendix A. According to Wang & al. (1990) the oil specific heat ratio is in the range of $C_{p_o}/C_{v_o} \approx (1.05 - 1.30)$. The results from Hysys for the different oils are in accordance with this (table 1-table 4), with some results outside of this range for some pressures and temperatures.

4 Speed of sound

4.1 Introduction

The speed of sound, also referred to as acoustic or sonic velocity can be defined as the characteristic speed of the propagation of infinitesimal pressure waves in a medium. The sound speed is usually expressed with Laplace equation:

$$a^2 = \frac{\partial p}{\partial \rho} \quad (19)$$

assuming an isentropic and reversible process. Danling & al. (2002) pointed out that this approximation will lead to errors in some cases. Saying this especially can not be neglected for the vapour-liquid two-phase in a non-isothermal process with phase transition. They further say that in such a case, the real process involves in heat transfer under temperature difference, friction by viscosity of the fluid and non-equilibrium phase transition between phases. In this work the authors also give an expression for acoustic velocity, taking into account these irreversible effects.

Defining the speed of sound in terms of specific volume and pressure gives this expression:

$$a = \sqrt{-v^2 \left(\frac{\partial p}{\partial v} \right)_s} \quad (20)$$

The compressibility is closely related to the speed of sound. Combining equation (20) with the definition of isentropic compressibility (17) gives this relation:

$$a = \sqrt{\frac{v}{c_s}} = \sqrt{\frac{1}{c_s \rho}} \quad (21)$$

4.2 NTNU sound speed model

A model for sound speed in multiphase mixtures was developed at Norwegian Institute of Technology (Dong and Gudmundsson, 1993). The authors list several analytical models for sound speed in gas-liquid mixtures based on equation (19). Instead of following this tradition, the authors relate the sonic velocity of the mixture directly to the properties of the gases and liquids. Combining equations (18) and (20) give an expression that relates the speed of sound to isothermal compressibility or the specific heat ratio, γ :

$$a^2 = \frac{\gamma}{c_T \rho} = \frac{C_p}{c_T \rho C_v} \quad (22)$$

To calculate the sound speed of a mixture arithmetically instead of differentially Dong and Gudmundsson (1993) gave a method to relate the relevant properties of a mixture to the properties of the mixture's components, presented below.

The density of a gas-liquid mixture is given by:

$$\rho_m = \alpha \rho_g + (1 - \alpha) \rho_l \quad (23)$$

The liquid phase can contain water and the liquid density is expressed by the oil and water densities like this:

$$\rho_l = \beta \rho_w + (1 - \beta) \rho_o \quad (24)$$

In the equations above α is the gas-liquid void fraction, and β is the water-oil volumetric fraction. Combining equations (23) and (24) gives the density of a gas-oil-water mixture:

$$\rho_m = \alpha \rho_g + (1 - \alpha) [\beta \rho_w + (1 - \beta) \rho_o] \quad (25)$$

Since α is the same as S_G in equation (14) and the liquid hold-up $(1 - \alpha)$ is the same as $S_o + S_w$, equation (14) can be written as:

$$c_m^T = \alpha c_g^T + (1 - \alpha) c_l^T \quad (26)$$

Again, if the liquid phase contains both water and oil, c_l can be expressed as:

$$c_l^T = \beta c_w^T + (1 - \beta) c_o^T \quad (27)$$

By combining equations (26) and (27) the isothermal compressibility of a gas-oil-water mixture can be expressed as:

$$c_m^T = \alpha c_g^T + (1 - \alpha) [\beta c_w^T + (1 - \beta) c_o^T] \quad (28)$$

The isobaric heat capacity for a gas-oil-water mixture can be expressed as:

$$C_p = x C_{p_g} + (1 - x) C_{p_l} = x C_{p_g} + (1 - x) [y C_{p_w} + (1 - y) C_{p_o}] \quad (29)$$

and the isochoric heat capacity:

$$C_v = x C_{v_g} + (1 - x) C_{v_l} = x C_{v_g} + (1 - x) [y C_{v_w} + (1 - y) C_{v_o}] \quad (30)$$

where x is the gas-liquid mass fraction and y is the water-oil mass fraction. By substituting equations (25), (28), (29) and (30) into equation (22) the sound speed in a gas-oil-water mixture is given as:

$$a = \sqrt{\frac{(x C_{p_g} + (1 - x) [y C_{p_w} + (1 - y) C_{p_o}]) / (x C_{v_g} + (1 - x) [y C_{v_w} + (1 - y) C_{v_o}])}{(\alpha \rho_g + (1 - \alpha) [\beta \rho_w + (1 - \beta) \rho_o]) \cdot (\alpha c_g^T + (1 - \alpha) [\beta c_w^T + (1 - \beta) c_o^T])}} \quad (31)$$

The properties needed to estimate the sound speed from equation (31) are isobaric and isochoric heat capacities, density and isothermal compressibilities for each of the constituents in the mixture. Dong and Gudmundsson (1993) gives relevant methods for evaluating these properties. Next chapter includes closer looks on the calculation of the oil properties.

4.3 Speed of sound in oils

The measured sound speed in various oils by Wang & al. (1990) is used by Dong and Gudmundsson (1993) to determine the isothermal oil compressibility. The acoustic velocity measurements have been made at the ultrasonic frequency of 800 kHz in eight dead oils and two refined hydrocarbons as well as one gas saturated oil (Wang & al., 1990). Gravity in these oils range from 0.73 to 1.037 g/cm³. An interpolation of the measured data has been used to estimate sound speed of an oil as a function of p, T and its API gravity (Dong and Gudmundsson, 1993).

From the interpolated velocity data, isentropic compressibility is found by rearranging equation (21):

$$c_o^s = \frac{1}{a^2 \rho} \quad (32)$$

which, since $\gamma=1$, is equal to the isothermal compressibility

In this study I have compared the Wang & al. velocity data to the oil velocities calculated from the compressibility correlations described in chapter 2. Isothermal compressibilities are estimated for four oils from Wang & al. (1990) using the three methods for undersaturated oils and related to acoustic velocity by equation NUM21; $a = \sqrt{1/c_s \rho}$ assuming isothermal and isentropic compressibilities are equal. The Vazquez and Beggs correlation, the Petrosky and Farshad correlation and the Al-Marhoun correlation is compared to the measured oil acoustic velocities this way.

4.4 Sound speed in dead oils

To compare the correlations to the dead oils in Wang & al. study, the bubble point pressure, (being an input parameter in all three models) was set to atmospheric conditions. The Vazquez and Beggs and the Petrosky and Farshad correlations were found to not be valid for bubblepoint pressures this low.

The results of using the Al-Marhoun correlation for three of these oils are shown in figures 1 to 7. As the plots show the Al-Marhoun correlation underpredicts the speed of sound in the oils compared to the measurements made by Wang & al. (1990). In the low-pressure region the difference is as much as 200 m/s, only decreasing some in the high-pressure region.

4.5 Sound speed in live oil

In addition to the ten dead oils Wang & al. (1990) also measured acoustic velocity in one gas-saturated (live) oil. The oil used was a recombined research fluid with bubblepoint at 206.4 bar at 71 °C. This reference does not give the density of the live oil, but the density of the dead end of it is given. The dead end of the fluid is the remainder of the live oil after the dissolved gases are out of solution (Wang & al., 1990). The dead end of the live oil is reported to have a density of 0.92 g/cm³ (23 °API). The presence of gas in the live oil will lead to a density slightly smaller than the dead end oil density. The acoustic velocities from the compressibility correlations were therefore calculated with oil densities ranging from 0.904 g/cm³ (25 °API to 0.876 g/cm³ (30 °API).

In figure 8 the sound speed from compressibility correlations is compared to the Wang & al. measured data for the live oil at 23 °C, assuming $\rho_o = 0.904 \text{ g/cm}^3$. The same conditions apply to the calculation in figure 9, except here the density is taken to be 0.876 g/cm³. Either way the calculated sound velocities are underestimated compared to the Wang & al. measurements. Al-Marhoun model (2003) underestimates the velocity with more than 200 m/s, as was roughly the same as for the dead oils. Acoustic velocities calculated from the Petrosky and Farshad compressibility correlation, is somewhat closer to the measurements but are also underestimated. For higher temperature (72°C) the results are the same, with underestimates of 200-300 m/s compared to the measurements, shown in figures 10 and 11.

When the pressure drops below the bubblepoint, acoustic velocities are expected to decrease significantly (Firoozabadi, 1999). In measurements made by Wang & al. (1990) this does not happen (figures 8-11).

4.6 Sound speed in oil under bubblepoint pressure

In this thesis, the acoustic velocities for the live oil at pressures lower than the bubblepoint pressure have been estimated from the compressibility correlation for saturated oils proposed by McCain & al. (1988). The estimation of velocity from compressibilities is made in the same manner as the three models above bubblepoint pressure. These calculations gave acoustic velocities in the range of 110-300 m/s. These results are not in correspondence with the measurements made by Wang & al. (1990). Wang & al. does not give any explanation of the unexpected behaviour of the acoustic velocity measurements. And at even lower pressures the signals from the speed measurements were lost.

5 Discussion

When comparing the sound speeds calculated from the oil compressibility correlations to the measurements of sound speeds in oils, a big disagreement is found. The heat capacities are assumed equal when equation N is used to calculate the sound speed from the isothermal compressibilities. According to Wang & al. (1990) C_p is a factor of 1.05-1.30 greater than C_v for oils. This is also backed up by Hysys data given in this thesis.

If this is applied to the calculation of sound speed from compressibility correlations, the isentropic compressibility should be used for the relation between compressibility and sound speed (equation N). Since isentropic compressibility is lower than the isothermal the sound velocity will become higher from applying $C_p/C_v > 1$ (from equations 18 and 21). The effect will not give much more satisfactory results when comparing to the measured oil acoustic velocities though, still underestimating the sound speed.

As a comment for the results from Hysys for heat capacity ratio I can say that they look a bit strange. The value for the heat capacity ratio suddenly takes a leap at a certain temperature when pressure is increased. Tables 1-4 show Hysys calculating the heat capacity ratio to values as high as 4-5. Wang & al. (1990) propose this ratio to be in the range 1.05-1.30 for oils.

Using isentropic compressibility as a starting point for estimating sound speeds in multiphase mixtures, as shown by Firoozabadi (2002) can be an alternative sound speed model.

6 Conclusion

Methods for estimating compressibility and sound speed in gases, oils, water and multiphase mixtures have been collected and studied. Some of these properties have been compared to properties used in NTNU multi-phase mixture sound speed model (Dong and Gudmundsson, 1993).

The Wang & al.'s (1990) measured sound velocities in oils have been compared to sound speed estimated from isothermal compressibility models for oil. The compressibility models underestimated the sound speeds in the area of 200 m/s, showing they are not good alternatives used in a sound speed model.

Nomenclature:

a	= acoustic velocity, sound speed
B	= formation volume factor
c, c_T	= isotherm compressibility
c_S	= isentropic compressibility
C_P	= isobaric heat capacity
C_V	= isochoric heat capacity
p	= pressure
R	= universal gas constant (8.3143 J/mol*K)
R_s	= solution gas-oil ratio
S	= saturation fraction
T	= temperature
V	= volume
v	= specific volume
x	= gas-liquid mass fraction
y	= water-oil mass fraction
z	= gas compressibility factor
α	= gas-liquid void fraction
β	= water-oil volumetric fraction
γ	= heat capacity ratio
γ_g	= gas specific gravity (air=1)
γ_o	= oil specific gravity (water=1)

Subscripts:

b	- bubblepoint
g	- gas
l	- liquid
m	- mixture, multi-phase
o	- oil
pc	- pseudo-critical
pr	- pseudo-reduced
S	- isentropic
T	- temperature, isothermal
w	- water

References

- Ahmed, T., (2001): “Reservoir Engineering Handbook” 2nd Edition, Elsevier, 1208
- Al-Marhoun, M.A., (2003): “The Coefficient of Isothermal Compressibility of Black Oils”, paper SPE 81432, 13th Middle East Oil Show & Conference, Bahrain, (5-8 April)
- Aspen Tech home page (2006): Aspen Hysys Product Detail, (www.aspentech.com)
- Calhoun Jr, J.C., (1947): “Fundamentals of Reservoir Engineering”, U of Oklahoma Press, Norman
- Danling, Z., Liangju, Z. and Yan, X., (2002): “The Influence of Irreversibility on Sound Velocity of Two-Phase Mixture”, 8th AIAA/ASME Joint Thermophysics and Heat Transfer Conference, St. Louis (24-26 June)
- Dong, L. and Gudmundsson, J.S., (1993): “Model for Sound Speed in Multiphase Mixtures”, 3rd Lerkendal Petroleum Engineering Workshop, Norwegian Institute of Technology, Trondheim, January 20-21
- Dranchuk, P.M. and Abou-Kassem, J.H., (1975): “Calculation of Z Factors For Natural Gases Using Equations of State”, The J of Can. Petrol. Tech., (July-September), p. 34-36
- Firoozabadi, A., (1999): “Thermodynamics of Hydrocarbon Reservoirs”, McGraw Hill,
- Firoozabadi, A., Nutakki, R., Wong, T.W. and Aziz, K., (1988): “EOS Predictions of Compressibility and Phase Behavior in Systems Containing Water, Hydrocarbons, and CO₂”, paper SPE 15674, Res. Eng., (May), 673-684
- Firoozabadi, A. and Pan, H., (2000): “Two-Phase Isentropic Compressibility and Two-Phase Sonic Velocity for Multicomponent-Hydrocarbon Mixtures”, paper SPE 65403, Reservoir Eval. & Eng. Vol. 3, No. 4, (August)

Ghedan, S.G., Aljawad, M.S., Poettmann, F.H. (1991): "Compressibility of Natural Gases", paper SPE 22234

Gudmundsson, J.S. and Celius, H.K. (1999): "Gas-Liquid Metering Using Pressure-Pulse Technology", paper SPE 56584, Annual Technical Conference and Exhibition, Houston, 3-6 October

McCain Jr, W.D., Rollins, J.B. and Villena Lanzi, A.J. (1988): "The Coefficient of Isothermal Compressibility of Black Oils at Pressures Below the Bubblepoint", paper SPE 15664

Muskat, M. (1949): "Physical principles of oil production" McGraw-Hill Book Co., p. 39.

Petrosky Jr, G.E. and Farshad, F.F., (1993): "Pressure-Volume-Temperature Correlations for Gulf of Mexico Crude Oils", paper SPE 26644

Ramey Jr, H.J., (1964): "Rapid Methods for Estimating Reservoir Compressibilities", paper SPE 772, JPT (April), p. 447-454

Trube, A.S., (1957): "Compressibility of Undersaturated Hydrocarbon Reservoir Fluids", Trans. AIME

Vazquez, M. and Beggs, H.D. (1980): "Correlations for Fluid Physical Property Prediction", paper SPE 6719, JPT (June), 968-970

Wang, Z., Nur, A.M. and Batzle, M.L. (1990): "Acoustic Velocities in Petroleum Oils", paper SPE 18163, JPT (February)

Whitson, C.H. and Brulé, M.R., (2000): "Phase behavior", SPE Monograph Volume 20

Tables

Table 1: C_p/C_v -values for Kristin reservoir fluid

C_p/C_v -values

from Hysys

Kristin T, (°C)	Total	Vapour	Liquid	Aqueous	Total	Vapour	Liquid	Aqueous	Total	Vapour	Liquid	Aqueous
	1000 kPa				3000 kPa				5000 kPa			
20	1,094	1,296	1,032	1,144	1,118	1,4	1,039	1,144	1,148	1,523	1,044	1,144
40	1,092	1,273	1,029	1,155	1,113	1,359	1,035	1,155	1,138	1,453	1,191	1,154
60	1,092	1,253	1,027	1,164	1,109	1,325	1,166	1,163	1,13	1,398	1,183	1,162
80	1,095	1,234	1,144	1,17								
100	1,103	1,217	1,14	1,175	1,107	1,269	1,161	1,174	1,122	1,319	1,186	1,172
120	1,126	1,206	1,13	1,18								
140												
160	1,139	1,178	1,127		1,145	1,22	1,127	1,189	1,137	1,247	1,137	1,187
180												
200	1,133	1,152	1,13		1,151	1,188	1,118		1,172	1,22	1,118	

T, (°C)	Total	Vapour	Liquid	Aqueous	Total	Vapour	Liquid	Aqueous
	7000 kPa				9000 kPa			
20	1,185	1,666	1,225	1,143	1,227	1,82	1,245	1,143
40	1,167	1,555	1,209	1,154	1,199	1,662	1,227	1,154
60	1,154	1,476	1,201	1,161	1,181	1,554	1,219	1,161
80								
100	1,14	1,369	1,212	1,171	1,161	1,417	1,238	1,17
120								
140								
160	1,144	1,275	1,147	1,185	1,156	1,303	1,151	1,183
180								
200	1,192	1,25	1,116	1,2	1,188	1,267	1,114	1,197

Table 2: C_p/C_v -values for Snorre reservoir fluid

C_p/C_v -values

from Hysys

Snorre T, (°C)	Total Vapour Liquid			Total Vapour Liquid			Total Vapour Liquid			Total Vapour Liquid			Total Vapour Liquid		
	p(kPa)			p(kPa)			p(kPa)			p(kPa)			p(kPa)		
	1000			2500			5000			7500			10000		
25	1,026	1,273	1,048	1,026	1,359	1,051	1,037	1,483	1,056	1,268		1,268	1,252		1,252
50	1,028	1,231	1,044	1,028	1,311	1,047	1,039	1,415	1,256	1,197	1,51	1,278	1,254		1,254
75	1,031	1,19	1,04	1,031	1,265	1,043	1,044	1,358	1,267	1,12	1,438	1,291	1,26		1,26
100	1,037	1,153	1,037	1,035	1,225	1,04	1,051	1,31	1,044	1,148	1,381	1,362	1,314		1,314
125	1,049	1,124	1,034	1,042	1,191	1,037	1,062	1,271	1,04	1,184	1,337	1,339	1,354		1,354
150	1,083	1,104	1,031	1,055	1,167	1,033	1,084	1,244	1,037	1,116	1,311	4,238	1,37		1,37

Table 3: C_p/C_v -values for Gullfaks reservoir fluid

C_p/C_v -values

from Hysys

Gullfaks T, (°C)	Total Vapour Liquid			Total Vapour Liquid			Total Vapour Liquid			Total Vapour Liquid			Total Vapour Liquid		
	p(kPa)			p(kPa)			p(kPa)			p(kPa)			p(kPa)		
	500			1500			2500			4000			5000		
10	1,018	1,302	1,017	1,02	1,35	1,018	1,023	1,398	1,019	1,027	1,475	1,021	1,03	1,532	1,022
20	1,018	1,293	1,017	1,02	1,338	1,018	1,022	1,381	1,019	1,026	1,449	1,02	1,029	1,498	1,144
40	1,017	1,275	1,016	1,019	1,315	1,017	1,021	1,351	1,158	1,025	1,405	1,151	1,028	1,442	1,149
80	1,017	1,233	1,203	1,018	1,272	1,18	1,02	1,3	1,169	1,023	1,337	1,159	1,026	1,362	1,155
160	1,016	1,147	1,25	1,017	1,188	1,191	1,019	1,211	1,172	1,022	1,237	1,156	1,024	1,252	1,149

Table 4: C_p/C_v -values for Oseberg reservoir fluid

C_p/C_v -values

from Hysys

Oseberg T, (°C)	Total Vapour Liquid			Total Vapour Liquid			Total Vapour Liquid			Total Vapour Liquid			Total Vapour Liquid		
	p(kPa)			p(kPa)			p(kPa)			p(kPa)			p(kPa)		
	500			2000			4000			10000			20000		
10	1,036	1,284	1,026	1,041	1,367	1,03	1,05	1,478	1,033	1,086	1,885	1,188	1,196		1,196
20	1,036	1,273	1,025	1,04	1,351	1,028	1,049	1,45	1,032	1,082	1,789	1,183	1,194		1,194
40	1,035	1,25	1,023	1,039	1,321	1,026	1,047	1,402	1,157	1,077	1,651	1,175	1,189		1,189
80	1,035	1,204	1,021	1,038	1,266	1,147	1,044	1,326	1,153	1,071	1,482	1,172	1,15	1,619	1,165
160	1,035	1,124	1,016	1,037	1,175	1,139	1,042	1,216	1,144	1,071	1,302	1,152	2,161	1,377	4,589

Figures

Figure 1: Sonic velocity vs pressure for dead oil I (0,73 g/cm³) at 23 °C

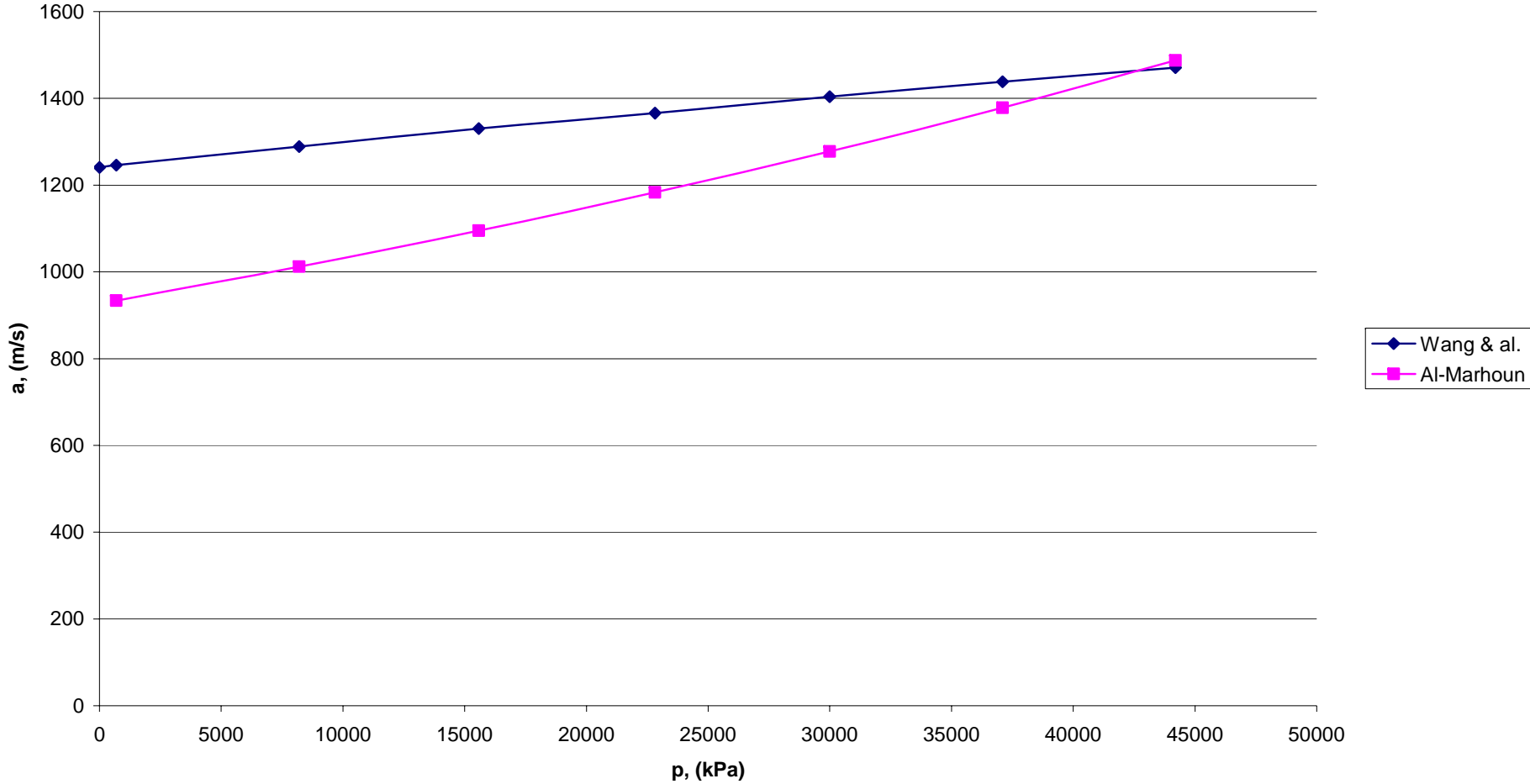


Figure 2: Sonic velocity vs pressure for dead oil I (0,73 g/cm³)
at 93 °C

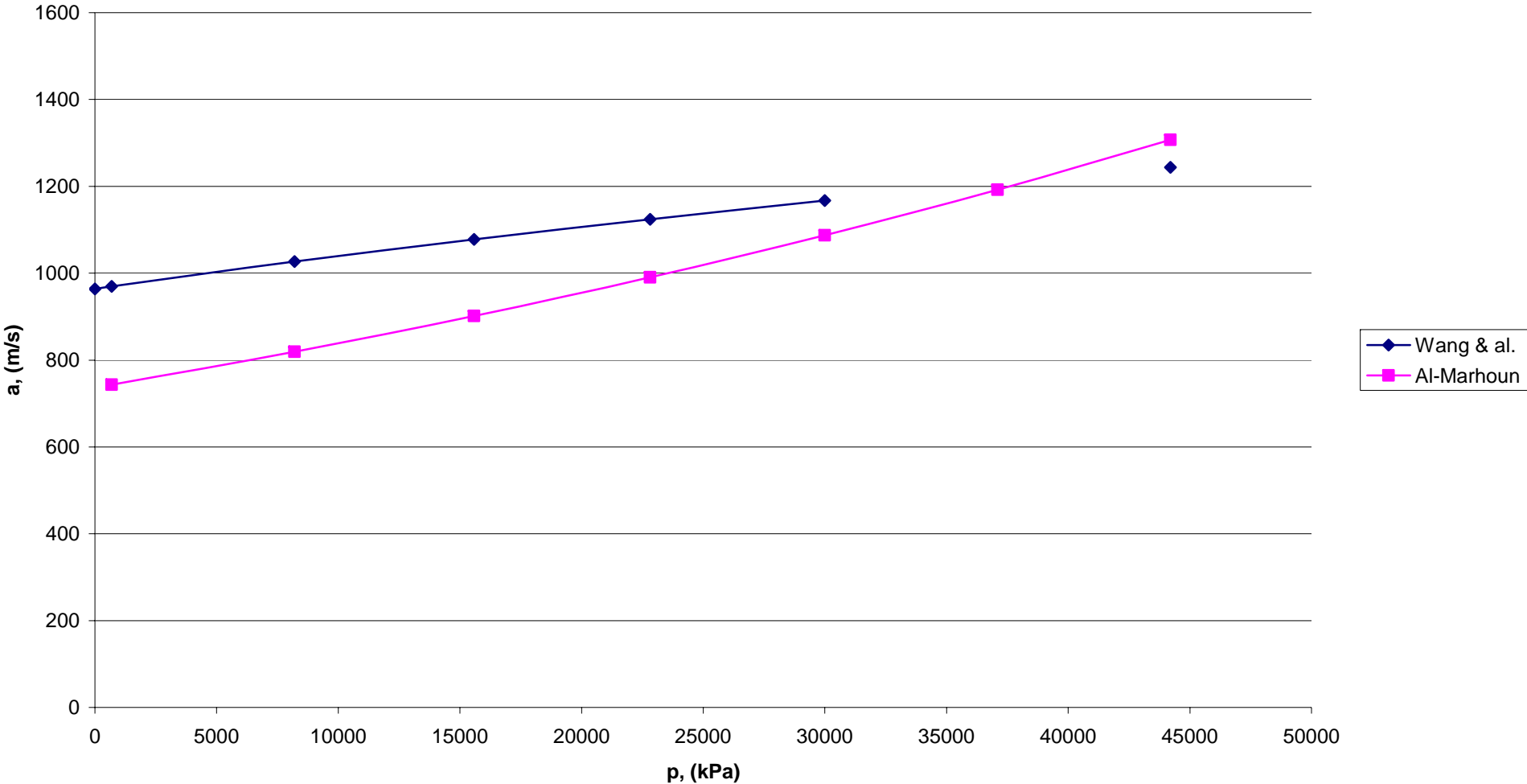


Figure 3: Sonic velocity vs pressure for dead oil G (0,8 g/cm³) at 24 °C

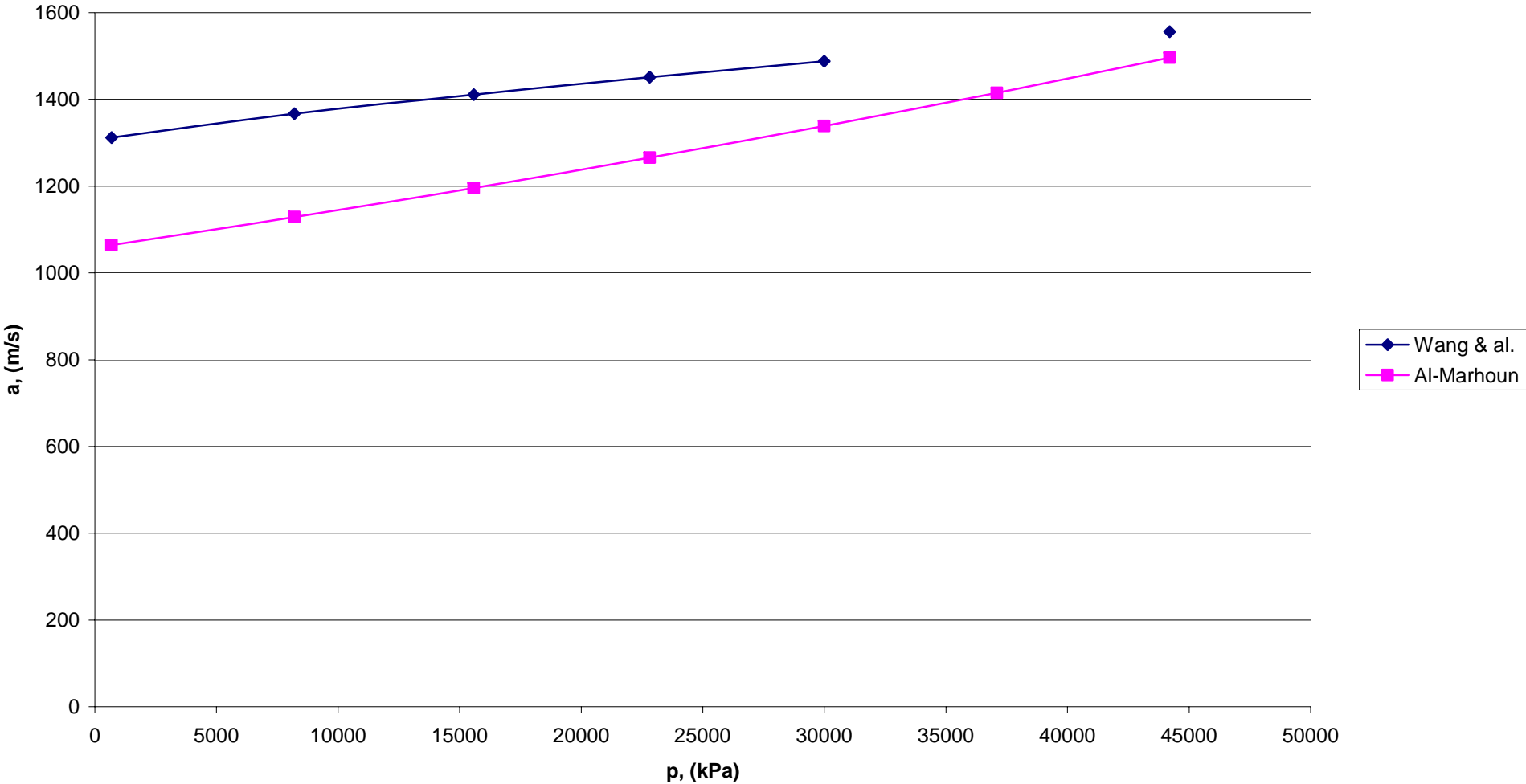


Figure 4: Sonic velocity vs pressure for dead oil G ($0,8 \text{ g/cm}^3$)
at $86 \text{ }^\circ\text{C}$

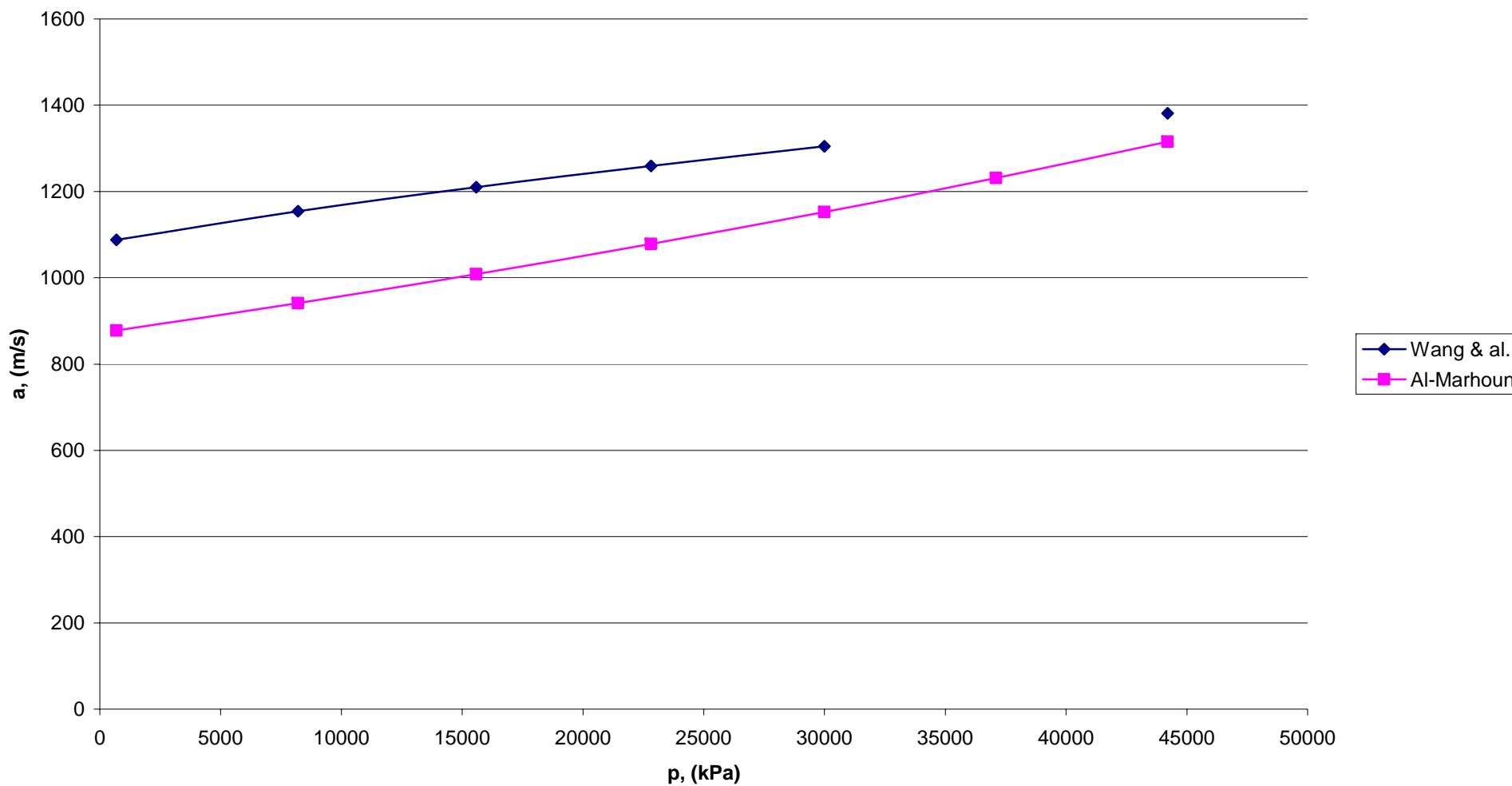


Figure 5: Sonic velocity vs pressure for dead oil D (0,996 g/cm³) at 21 °C

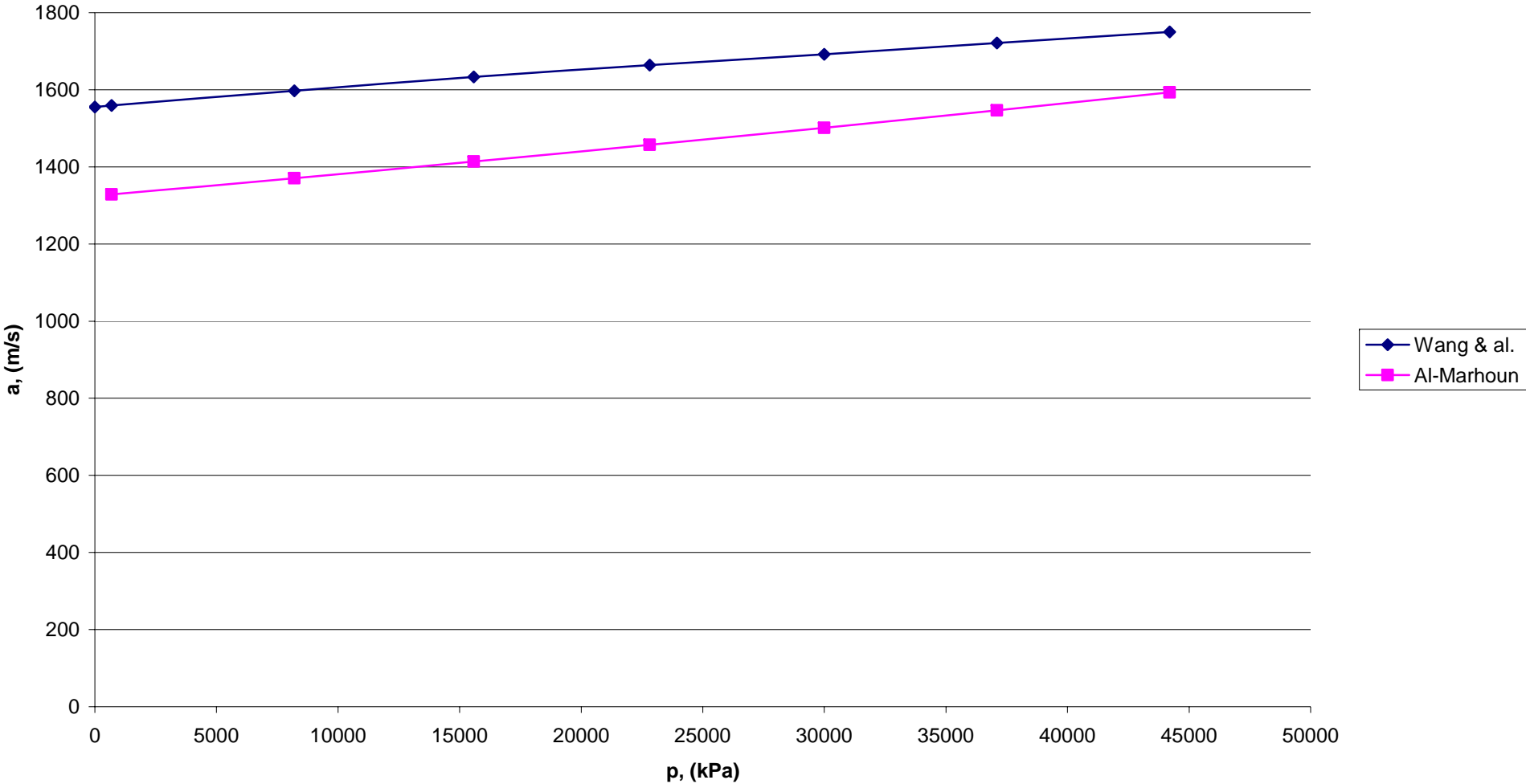


Figure 6: Sonic velocity vs pressure for dead oil D (0,996 g/cm³) at 63 °C

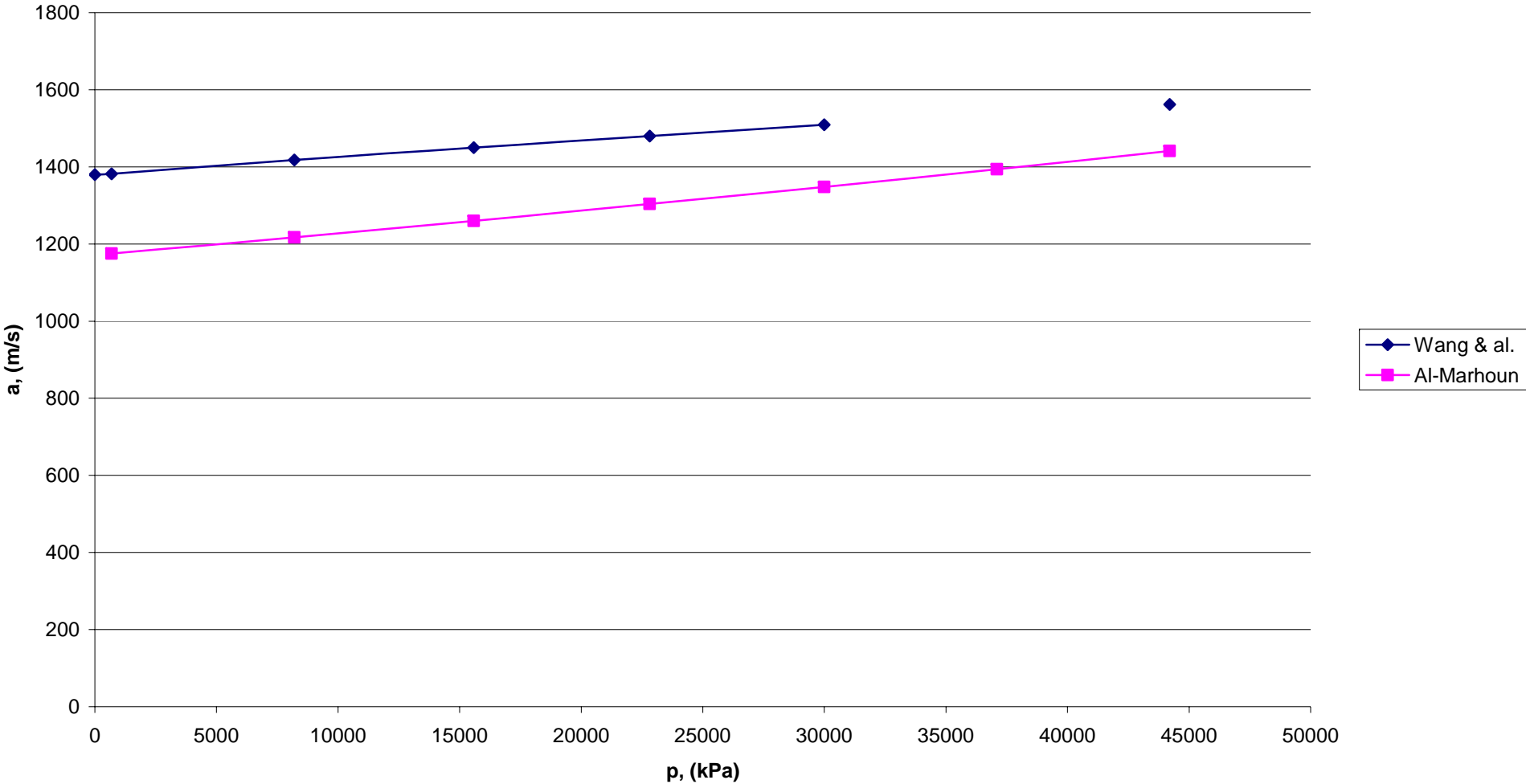


Figure 7: Sonic velocity vs pressure for dead oil D (0,996 g/cm³) at 114 °C

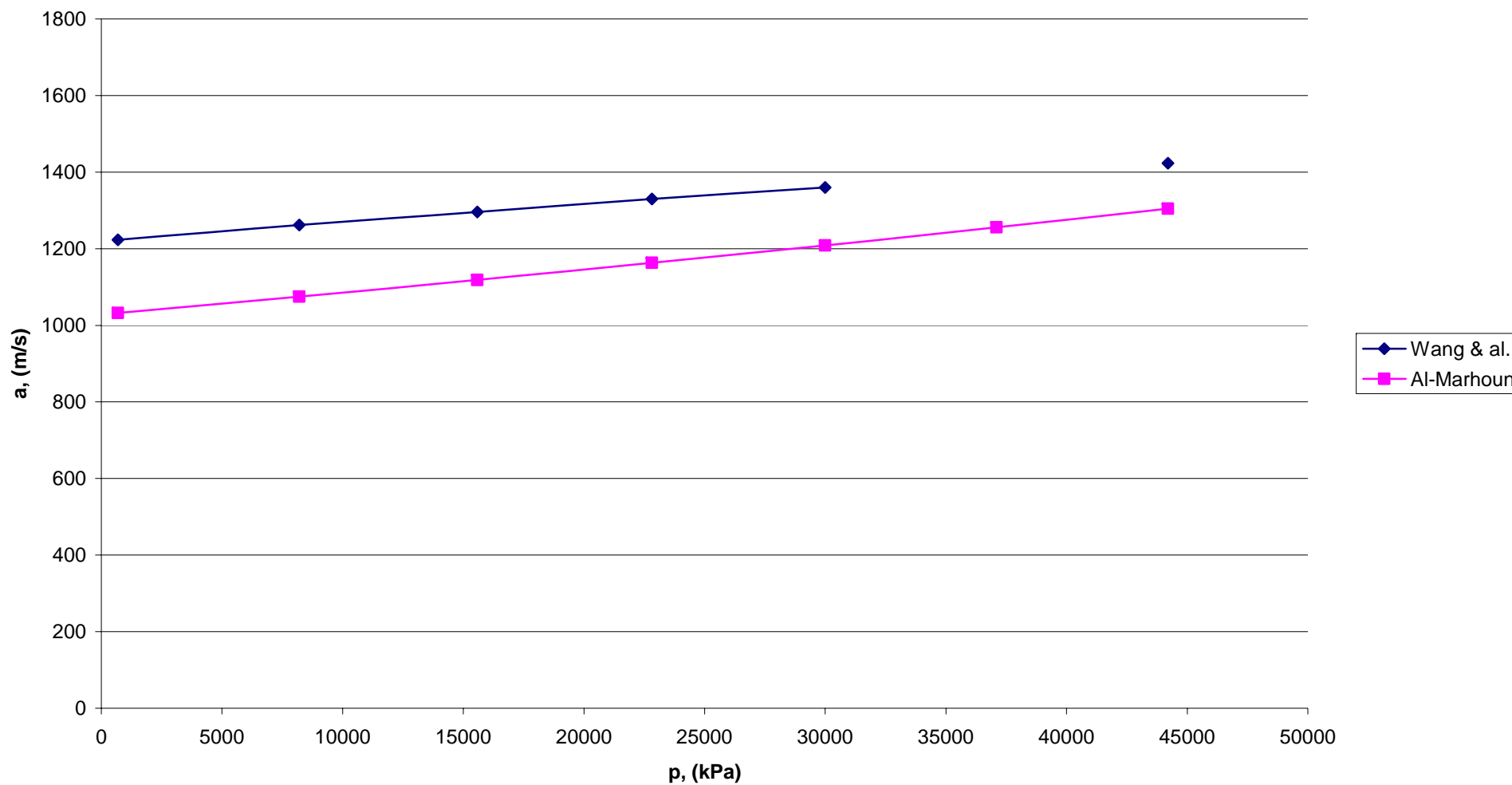


Figure 8: Sonic velocity vs pressure in live oil ($\rho_o=0.904 \text{ g/cm}^3$) at 23°C

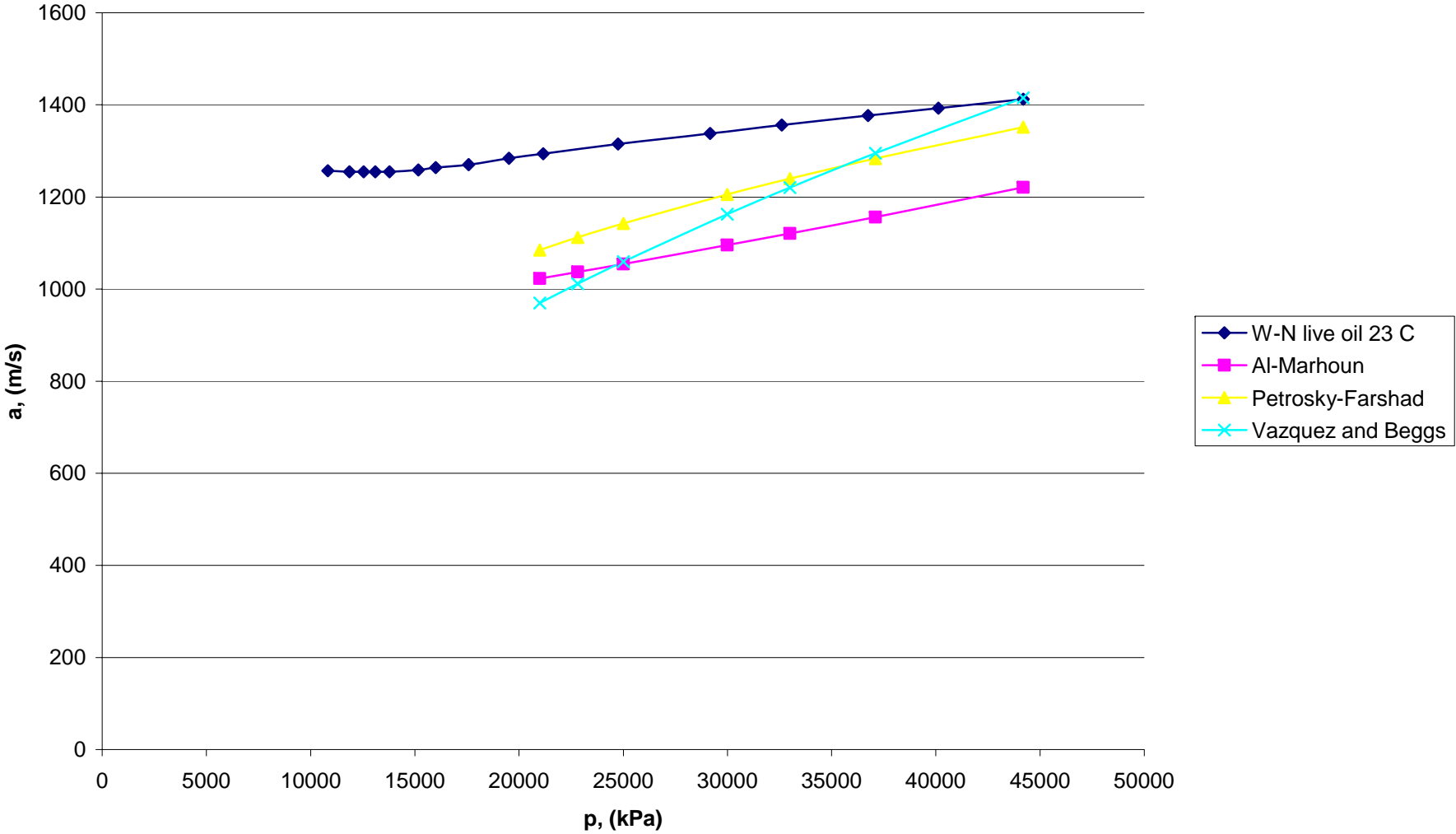


Figure 9: Sonic velocity vs pressure in live oil ($\rho_o=0.876 \text{ g/cm}^3$) at 23°C

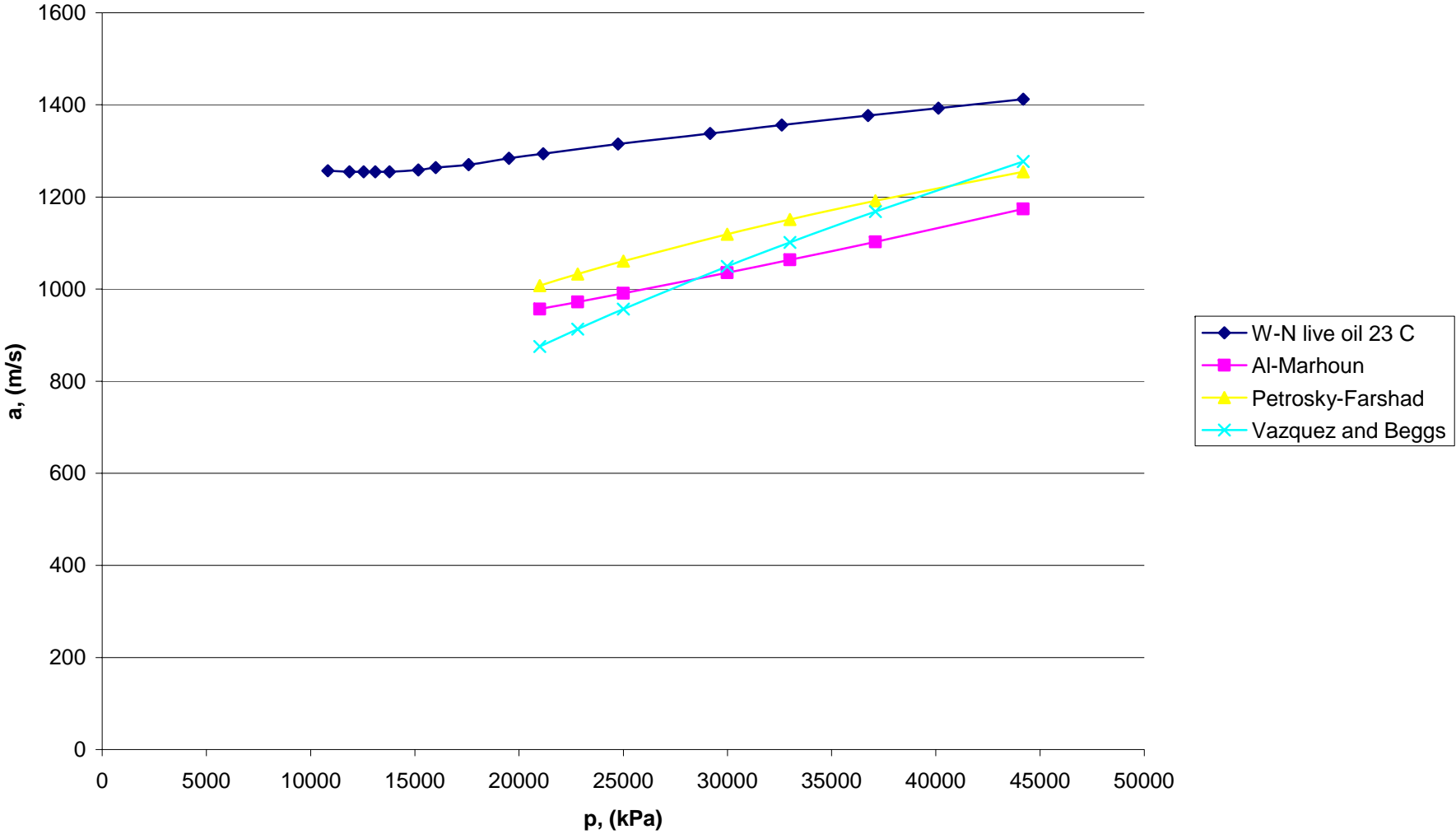


Figure 10: Acoustic velocity vs pressure in live oil ($\rho_o=0.904\text{g/cm}^3$)
at 72°C

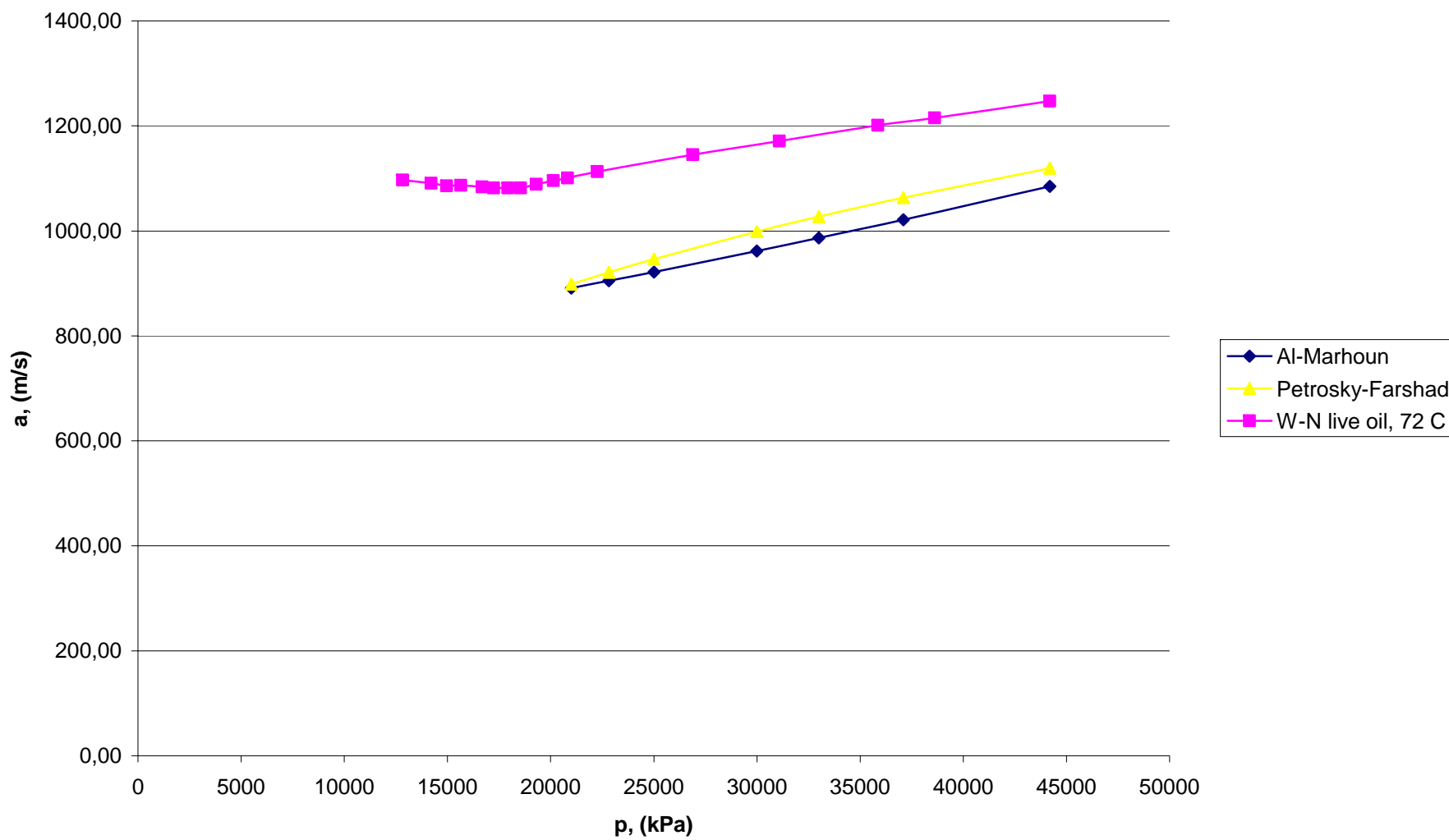
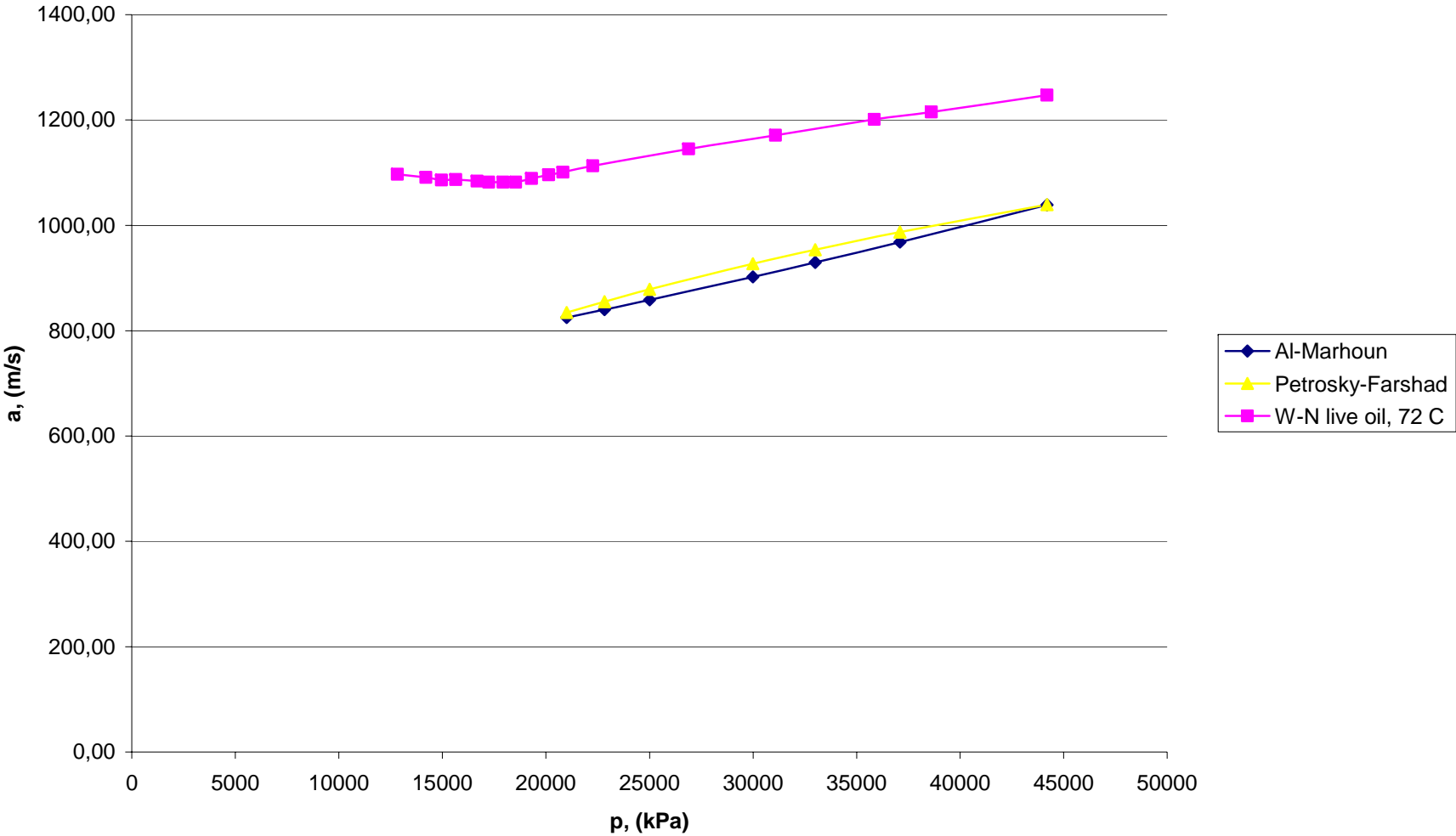


Figure 11: Acoustic velocity vs pressure in live oil ($\rho_0=0.876\text{g/cm}^3$) at 72°C



Appendix A: Fluid compositions used in Hysys for simulation of C_p/C_c -ratio in oils

Reservoir fluid compositions

Component	Snorre	Kristin	Oseberg	Gullfaks
H2O	not incl.	0,2479	not incl.	
Nitrogen	0,0117	0,0023	0,00360	0,0031
CO2	0,0012	0,0252	0,00650	0,0100
Methane	0,2524	0,5200	0,50668	0,4633
Ethane	0,0705	0,0655	0,05619	0,0404
Propane	0,0809	0,0321	0,03779	0,0088
i-Butane	0,0124	0,0065		0,0056
n-Butane	0,0504	0,0117	0,02679	0,0051
i-Pentane	0,0197	0,0043		0,0066
n-Pentane	0,0301	0,0045	0,02010	0,0029
Hexane	0,0383	0,0071	0,01910	0,0101
Heptane	0,4324	0,0117	0,03649	0,0287
Octane		0,0127	0,04019	0,0406
Nonane		0,0083	0,02829	0,0326
Decane		0,0207	0,01440	0,3422
C11			0,01950	
C12			0,01860	
C13			0,01960	
C14			0,01590	
C15		0,0150	0,01610	
C16			0,01210	
C17			0,01210	
C18			0,01020	
C19			0,01020	
C20			0,06958	
C25		0,0045		
Sum	1,0000	1,0000	1,00000	1,0000

Appendix B: Hysys simulation tool

Aspen Hysys is a process modelling tool for steady state simulation, design, performance monitoring, optimization and business planning for oil & gas production, gas processing and petroleum refining industries. Hysys is built upon proven technologies, with more than 25 years experience supplying process simulation tools to the oil & gas and refining industries. It provides an intuitive and interactive process modeling solution that enables engineers to create steady state models for plant design, performance monitoring, troubleshooting, operational improvement, business planning and asset management. (Aspen Tech, 2006)

My simulations in Hysys, were quite ordinary with few or no process equipment involved. The simulations were on one stream, giving the properties from the componential input of hydrocarbon mixtures shown in appendix A.

The components of the relevant fluid were added in Hysys for the simulations. Fluid/thermodynamic package was chosen, Peng-Robinson EOS was used in all simulations.

Appendix C: Wang & al. (1990) measured acoustic velocities (m/s) in selected oils at different temperatures and pressures.

Table C1: Wang & al. Oil I

		<u>62°API = 731kg/m³</u>					
		T (°C)					
p (psig)		23	44	64	85	93	109
0		1241	1155	1077	997	964	897
100		1246	1159	1082	1004	970	904
1190		1289	1204	1133	1060	1027	967
2260		1330	1246	1181	1111	1078	1023
3310		1366	1287	1223	1156	1124	1074
4350		1404	1326	1262	1199	1167	1119
5380		1438					
6410		1471	1393	1333	1274	1244	1202

Table C2: Wang & al. Oil G

		<u>43°API = 811kg/m³</u>			
		T (°C)			
p (psig)		24	42	62	86
0					
100		1312	1245	1170	1088
1190		1367	1297	1229	1154
2260		1411	1346	1280	1210
3310		1451	1388	1327	1259
4350		1488	1427	1368	1305
5380					
6410		1556	1508	1447	1381

Table C3: Wang & al. Oil D

		<u>10,5°API = 996kg/m³</u>						
		T (°C)						
p (psig)		21	30	40	63	84	104	114
0		1555	1507	1473	1380	1309	1247	
100		1559	1510	1477	1382	1311	1252	1223
1190		1597	1546	1508	1418	1346	1290	1262
2260		1633	1577	1541	1450	1380	1324	1296
3310		1664	1610	1571	1480	1413	1356	1330
4350		1692	1643	1600	1509	1441	1388	1360
5380		1721						
6410		1750	1694	1656	1562	1496	1447	1423

Table C4: Wang & al. Live oil (gas saturated)

Live oil					
p, (psi)	23°C		72°C		
	p, (kPa)	a (m/s)	p, (psi)	p, (kPa)	a (m/s)
1570	10825	1257	1860	12824	1097
1720	11859	1255	2060	14203	1091
1820	12548	1255	2170	14962	1086
1900	13100	1255	2270	15651	1087
2000	13790	1255	2420	16685	1084
2200	15168	1259	2500	17237	1082
2320	15996	1264	2600	17926	1082
2550	17582	1270	2690	18547	1082
2830	19512	1284	2800	19305	1089
3070	21167	1294	2920	20133	1096
3590	24752	1315	3020	20822	1101
4230	29165	1338	3230	22270	1113
4730	32612	1356	3900	26890	1145
5330	36749	1377	4510	31095	1171
5820	40127	1393	5200	35853	1201
6410	44195	1412	5600	38611	1215
			6410	44195	1247

Appendix D: Excel spreadsheets

Appendix D1: Excel spreadsheet calculating oil isothermal compressibility from correlations

Oil gravity	$\gamma_o=$	10,5	°API	0,996	g/cm3					
Gas gravity	$\gamma_g=$	0,7	(air=1)							
Temperature	T=	114	°C	237,2	°F					
Bubblepoint pressure	pb=	14,696	psi							
Pressure	p=	690	8205	15582	22822	29992	37094	44195	kPa	
		100,08	1190,03	2259,98	3310,05	4349,97	5380,03	6409,94	psi	
Standing correlation	$R_{sb}=$	1,438							scf/STB	
Vazquez and Beggs										
γ_s corrugated	$\gamma_{gs}=$	0,693895	0,804720	0,833430	0,850512	0,862741	0,872254	0,880095		
Solubility GOR	$R_{sb}=$	0,700							scf/STB	
Using V-B Rs	$c_o=$	1,962E-04	1,540E-05	7,962E-06	5,375E-06	4,057E-06	3,259E-06	2,721E-06	psi ⁻¹	
Petrosky-Farshad										
	$R_{sb}=$	36,626							scf/STB	
Using P-F Rs	$c_o=$	1,092E-05	2,530E-06	1,732E-06	1,382E-06	1,176E-06	1,038E-06	9,357E-07	psi ⁻¹	
Al-Marhoun										
Oil FVF	$B_{ob}=$	1,0942							RB/STB	
γ_o at bubblepoint	$\gamma_{ob}=$	0,9109								
Compressibility	$c_o=$	6,490E-06	5,986E-06	5,530E-06	5,115E-06	4,736E-06	4,387E-06	4,065E-06	psi ⁻¹	

Appendix D2: Excel spreadsheet for calculating sound speed in oils from compressibility correlations

Oil gravity	$\gamma_o =$	10,5	°API	0,996	g/cm ³	996	kg/m ³	
Temperature	T=	114	°C	237,2	°F			
Conversion factor		6,894757	kPa/psi					
Pressure, [kPa]		690	8205	15582	22822	29992	37094	44195
	[psi]	100,1	1190,0	2260,0	3310,1	4350,0	5380,0	6409,9
Compressibilities, [1/psi]								
Vazquez and Beggs	1,966E-04	1,544E-05	7,978E-06	5,386E-06	4,065E-06	3,266E-06	2,727E-06	
Petrosky-Farshad	1,156E-06	2,678E-07	1,834E-07	1,464E-07	1,246E-07	1,099E-07	9,907E-08	
Al-Marhoun	6,490E-06	5,986E-06	5,530E-06	5,115E-06	4,736E-06	4,387E-06	4,065E-06	
Compressibilities, [1/kPa]								
Vazquez and Beggs	2,852E-05	2,239E-06	1,157E-06	7,812E-07	5,896E-07	4,737E-07	3,955E-07	
Petrosky-Farshad	1,676E-07	3,884E-08	2,660E-08	2,123E-08	1,807E-08	1,594E-08	1,437E-08	
Al-Marhoun	9,414E-07	8,683E-07	8,020E-07	7,419E-07	6,869E-07	6,363E-07	5,895E-07	
Sound/sonic velocity, [m/s]								
Vazquez and Beggs	187,59	669,52	931,28	1133,41	1304,60	1455,49	1592,91	
Petrosky-Farshad	2446,73	5082,77	6142,63	6875,35	7453,03	7935,76	8357,03	
Al-Marhoun	1032,50	1075,08	1118,60	1163,02	1208,74	1255,81	1304,70	